Nd3+ concentration effect on luminescent properties of MgAl2O4 nanopowders synthesized by modified Pechini method

Golyeva E.V., Vaishlia E.I., Kurochkin M.A., Yu Kolesnikov E., Lähderanta E., Semencha A.V., Kolesnikov I.E.

DOI: 10.1016/j.jssc.2020.121486

Nd^{3+} concentration effect on luminescent properties of $MgAl_2O_4$ nanopowders synthesized by modified Pechini method

E.V. Golyeva[*,a], E.I. Vaishlia[a], M.A. Kurochkin[b], E.Yu. Kolesnikov[c], E. Lähderanta[d], A.V. Semencha[a], I.E. Kolesnikov[b,d]

[a]*Peter the Great St. Petersburg Polytechnic University, Polytechnicheskaya 29, 195251, St. Petersburg, Russia*

[b]*St. Petersburg State University, Universitetskaya nab. 7/9, 199034, St. Petersburg, Russia*

[c]*Volga State University of Technology, Lenin sqr. 3, Yoshkar-Ola 424000, Russia*

[d]*LUT University, Skinnarilankatu 34, 53850, Lappeenranta, Finland*

Contact information

e-mail address: golieva_ev@spbstu.ru (E. Golyeva)

Abstract

In this paper, a concentration series of $MgAl_2O_4:Nd^{3+}$ nanocrystalline powders have been synthesized by modified Pechini method. Neodymium doping concentration was varied within range of 0.05–5 at.%. The obtained samples have been analyzed using the various experimental methods: X-Ray diffraction, scanning electron microscopy, energy dispersive X-Ray spectroscopy, as well as steady-state and kinetics photoluminescence spectroscopy. According to XRD, all synthesized samples are monophasic without any structural impurities. The doping concentration effect on the luminescent characteristics of $MgAl_2O_4:Nd^{3+}$ nanocrystalline particles has been studied in terms of emission intensity and lifetime. The optimal doping Nd^{3+} concentration was determined to be 0.1 at.%. Concentration quenching in $MgAl_2O_4:Nd^{3+}$ powders occurred via energy transfer among the nearest neighbor ions. Performed studies shed the light on behavior of Nd^{3+} ions in nanoscale magnesium aluminum spinel.

Keywords: neodymium, $MgAl_2O_4$, luminescence, concentration quenching, lifetime, nanopowders

1. Introduction

At present time, the study and production of nanoparticles are relevant in the fields of medicine, biology and the semiconductor industry [1–7]. Recently, aluminate phosphors, for example magnesium aluminum spinel (MAS), doped with rare earth ions (RE^{3+}) became widespread [8–11]. Proper choice of doping ion is crucial to obtain specific properties for particular utilization.

Magnesium aluminum spinels doped with neodymium ions have wide application due to their unique features. One of such properties is the availability of transparency windows that allows using the material as thermal indicators [12]. Another feature is the implementation of inter-level transitions in the 4f shell, whose electrons are shielded from external influences [13]. The nature of the excitation and emission spectra for neodymium ions remains independent of the nanocrystalline host, because the crystal field effect of the host is significantly weaker than subatomic interactions [14]. Despite the fact that Nd^{3+} introduction in different host weakly affects the energy levels position, the emission intensity highly depends on certain host [15]. Magnesium aluminum spinel has a high hardness, high melting point (T = 2135 ° C), a wide spectral transmission of electromagnetic radiation (200-5500 nm), ease of fabrication and crystal size capability [16–19]. Along the $MgAl_2O_4$: RE^{3+}, similar host lattices such as $ZnAl_2O_4$ spinels

doped with lanthanides have been studied in [20,21] The concentrations effect on the luminescent properties of Eu^{3+} [20] and Tb^{3+} [21] were investigated. It was also shown that the lattice type of spinel (normal or inverse) affects luminescence properties and Tb^{3+} ions can be used as an optical probe to evaluate the fractional population of the inverse and normal spinel structures in $ZnAl_2O_4$ [21]. MAS doped with Eu^{3+} has bright red fluorescence and was studied by many groups, including ours [10,11,22]. The MAS:Eu^{3+} nanoceramic was even obtained and differences between nanopowders and ceramic spinels were investigated [23]. Conducted analysis of the literature showed that neodymium spinel has been less studied unlike MAS with europium.

Magnesium aluminum spinel doped with neodymium has been explored by P.J. Deren et al. [24]. Synthesis of the concentration series $MgAl_2O_4:Nd^{3+}$ allowed to establish the empirical dependence of the size of particle agglomerates on the doping concentration. Increase of Nd^{3+} doping concentration resulted in broadening of emission bands, which was associated with a decrease of the average nanoparticles size from 12 nm to 7 nm. However, authors did not provide study of concentration effect at room temperature. Another study in this area was related to the investigation of structural and spectroscopic properties of $MgAl_2O_4:Nd^{3+}$ ceramics produced by two-stage spark plasma sintering [25]. The authors used commercial MAS powder and added Nd^{3+} (0.1 or 0.2 at.%) by impregnation of $MgAl_2O_4$ pressed pellets into neodymium nitrate hexahydrate water solution. The used method has a disadvantage compared to the modified Pechini method because of inhomogeneous doping ion distribution in host. Low rare earth equilibrium solubility in MAS is one of the main difficulties on the route to produce efficient doped spinel for photonic purpose. Therefore, the study of doping concentration effect on $MgAl_2O_4:Nd^{3+}$ structural and luminescent properties and development of special manufacturing technique to promote neodymium solubility in spinel host is in high demand.

In this work, the synthesis aluminum magnesium spinel doped with neodymium was carried out by a modified Pechini method for a series of concentrations 0.05 at.%, 0.1 at.%, 0.5 at.%, 1 at.%, 2 at.%, 5 at.%. The main aims were to study the doping concentration effect in $MgAl_2O_4:Nd^{3+}$ samples on steady-state and kinetics photoluminescence characteristics at room temperature and to define the mechanism of luminescence concentration quenching.

2. Experimental

The $MgAl_2O_4:Nd^{3+}$ samples have been synthesized by modified Pechini method [26–29]. Doping concentration of Nd^{3+} was controlled from 0.05 to 5.0 at.% in respect to appropriate Mg^{2+} atomic content. The technique of synthesis Pechini method involves the dissolution of stoichiometric amounts of magnesium nitrate $Mg(NO_3)_2•6H_2O$ (99%), aluminum nitrate $Al(NO_3)_3•9H_2O$ (99,999%) in water and stoichiometric amount of neodymium oxide Nd_2O_3 (99,999%) in 5 ml concentrated nitric acid (65%). Obtained solutions were mixed with 12 ml citric acid for formation of citrate complex $[Me(C_6H_8O_7)_3](NO_3)_3$ and then with 3 ml ethylene glycol for gelation. Modified Pechini method includes two stages of calcination. During the first calcination, organic compounds were removed at a temperature of 600 °C for a 1 hour. The second calcination was carried out with powder after the first calcination, which was ground with potassium chloride (in weight ratio 1:1). The experimental parameters of the second calcination were 950°C for the temperature and 4 hours as duration. After this, nanopowder with KCl was centrifuged with water three times for removal of the salt until $MgAl_2O_4:Nd^{3+}$ was purified. The proposed modification of Pechini technique allows to obtain finely dispersed nanoparticles with different compositions [26–29].

The study of MAS:Nd^{3+} powders was carried out using various experimental methods, such as X-Ray diffraction, scanning electron microscopy, energy dispersive X-Ray spectroscopy, and photoluminescence spectroscopy. Structure measurements were performed at X-ray diffractometer D8 Advance Bruker AXS with radiation Cu-Kα1 (wavelength λ =1.54 Å) in the range from 10 to 80°. The morphology was studied with a SUPRA 40VP WDS scanning electron microscope (shooting mode: I= 10 mA, U=30 kV). The elemental composition was investigated by energy dispersive X-ray spectral spectroscopy (EDX). The synthesized powders (5 mg) and potassium bromide (300 mg) were pressed into pellets (diameter 13 mm) for luminescence studies. Photoluminescence spectra were measured on fluorescence spectrometer Fluorolog-3 equipped with a Xe-arc lamp (450 W power) with typical slit width of 10 nm. Kinetics measurements were carried out on the same device with pulsed Xe-lamp (150 W power, 3 μs pulse width) as an excitation source. All photoluminescence studies were performed at room temperature.

3. Results and discussion

The XRD patterns of $MgAl_2O_4$:xNd^{3+} (0.05<x<5 at.%) powders as well as $MgAl_2O_4$ reference standard are presented in Fig. 1. The experimental peaks match well with reference standard, therefore it can be concluded that all synthesized samples have pure cubic phase without any structural impurities. According to the results of X-Ray phase analysis, $MgAl_2O_4$:Nd^{3+} characteristic space group symmetry is Fd-3m. The unit-cell lattice parameter, crystal cell volume, and the average size of coherent scattering region (CSR) were calculated by Rietveld refinement analysis using Bruker TOPAS 4.2 software. The crystal cell volume of MAS:Nd^{3+} 0.1 at.% was determined to be (520±2) $Å^3$, while lattice parameter was 8.04 Å. The crystallite size (CRS) of $MgAl_2O_4$:Nd^{3+} does not change significantly with the increasing of Nd^{3+} concentration and amounts to 6.6 nm for 0.05% Nd^{3+}, 7.4 nm for 0.1% Nd^{3+} and 5.6 nm for 5% Nd^{3+}.

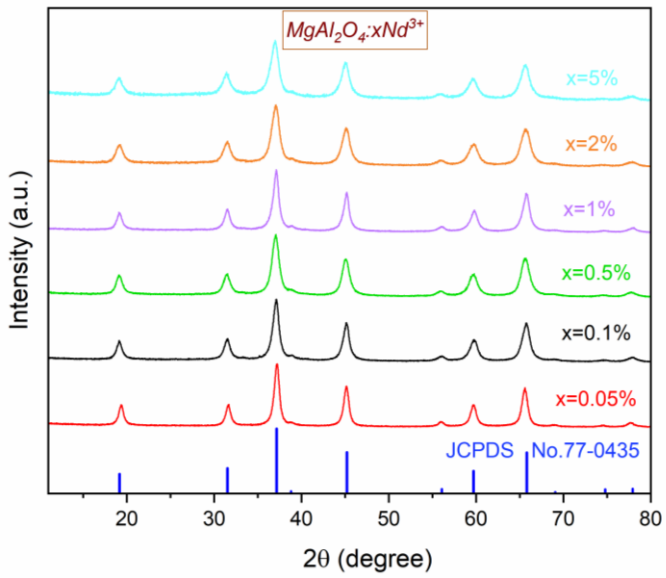

Fig. 1. The diffraction patterns of $MgAl_2O_4$:xNd^{3+} (0.05<x<5 at.%) and $MgAl_2O_4$ reference standard (JCPDS 77-0435)

The SEM image of the $MgAl_2O_4$:Nd^{3+} 0.1 at.% sample was obtained to determine the morphology of the synthesized particles (Fig. 2a). As can be seen, prepared powder consisted of

spherical particles, whose average size was less than 100 nm. EDX was performed to determine the elemental composition of spinel sample (Fig. 2b). EDX spectrum included peaks of Mg (16.23%), Al (32.08%), and O (51.68%) elements, whereas neodymium was not detected. This fact is explained by very small concentration of Nd^{3+} ions in the $MgAl_2O_4$ host (0.1 at.%). Presence of neodymium in synthesized powders was clearly seen by photoluminescence studies.

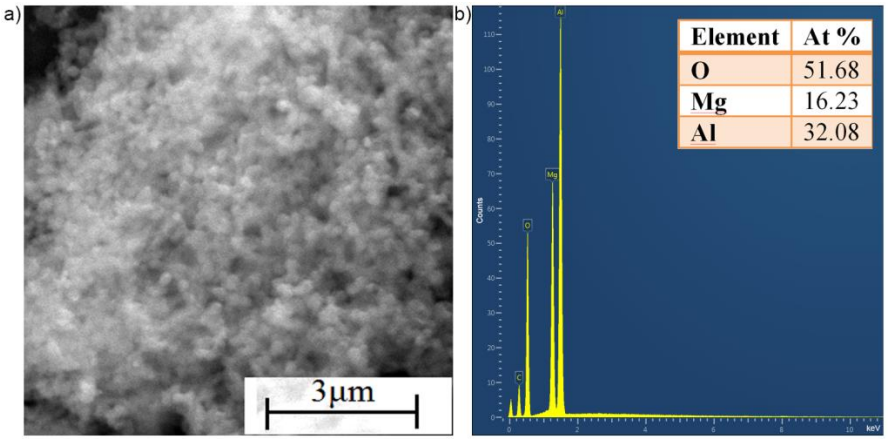

Fig. 2. a) SEM image and b) EDX spectrum of MAS:Nd^{3+} 0.1 at.% nanocrystalline powder

Fig. 3a shows emission spectra of nanocrystalline $MgAl_2O_4$:Nd^{3+} concentration series upon 584 nm excitation. The observed spectra include characteristic bands corresponding to the transitions originated from excited $^4F_{3/2}$ level: $^4F_{3/2} – {}^4I_{9/2}$ (850–990 nm), $^4F_{3/2} – {}^4I_{11/2}$ (1020–1200 nm) and $^4F_{3/2} – {}^4I_{13/2}$ (1300–1465 nm). Each emission transition of Nd^{3+}-doped phosphors usually consists of several narrow well-resolved lines corresponding to the Stark splitting of excited and ground levels due to crystal field [28,29]. However, the unresolved broad emission peaks were detected in case of $MgAl_2O_4$:Nd^{3+} nanopowders. This fact can be elucidated by the multisite distribution of Nd^{3+} ions in spinel structure, which leads to the line broadening [30,31].
Emission spectra are dominated by $^4F_{3/2} – {}^4I_{11/2}$ transition centered at 1075 nm. The integral intensity of this transition calculated within 1020–1200 nm boundaries as a function of Nd^{3+} concentration was plotted in Fig. 3b to define optimal doping concentration. There are two competitive effects occurring along with increase of the doping concentration, which influence on the optimum doping concentration value: growth of radiative recombination and growth of nonradiative decay rate (energy transfer) [32]. As can be seen, emission intensity goes up for weakly-doped samples (0.05 and 0.1 at.%), but further increase of Nd^{3+} doping ions results in intensity reduction due to the concentration quenching effects. The optimum Nd^{3+} concentration was found to be 0.1 at.% in $MgAl_2O_4$ host.
Fig. 3c presents excitation spectra of nanocrystalline $MgAl_2O_4$:Nd^{3+} concentration series monitored at the most intensive transition $^4F_{3/2} – {}^4I_{11/2}$ (λ_{em} = 1075 nm). The obtained spectra consist of intense band in the UV region and several lines in visible and IR regions. The broad band can be attributed to the charge transfer transition (CT) between O^{2-} and Nd^{3+} ions. Longer wavelength peaks correspond to intra-configurational f-f transitions from ground level $^4I_{9/2}$. The observed excitation lines centered at 357, 433, 474, 528, 584, 685, 746, and 807 nm can be assigned to $^4I_{9/2} – {}^4D_{3/2} + {}^4D_{1/2}$, $^4I_{9/2} – {}^2D_{5/2}$, $^4I_{9/2} – {}^4G_{9/2} + {}^4G_{11/2} + {}^2K_{15/2}$, $^4I_{9/2} – {}^4G_{7/2} + {}^4G_{9/2} + {}^2K_{13/2}$, $^4I_{9/2} – {}^4G_{5/2} + {}^4G_{7/2} + {}^2H_{11/2}$, $^4I_{9/2} – {}^4F_{9/2}$, $^4I_{9/2} – {}^4F_{7/2} + {}^4S_{3/2}$, and $^4I_{9/2} – {}^4F_{5/2}$ transitions, respectively [33]. The most efficient direct Nd^{3+} excitation can be provided through $^4I_{9/2} – {}^4G_{5/2} + {}^4G_{7/2} + {}^2H_{11/2}$ transition (584 nm).

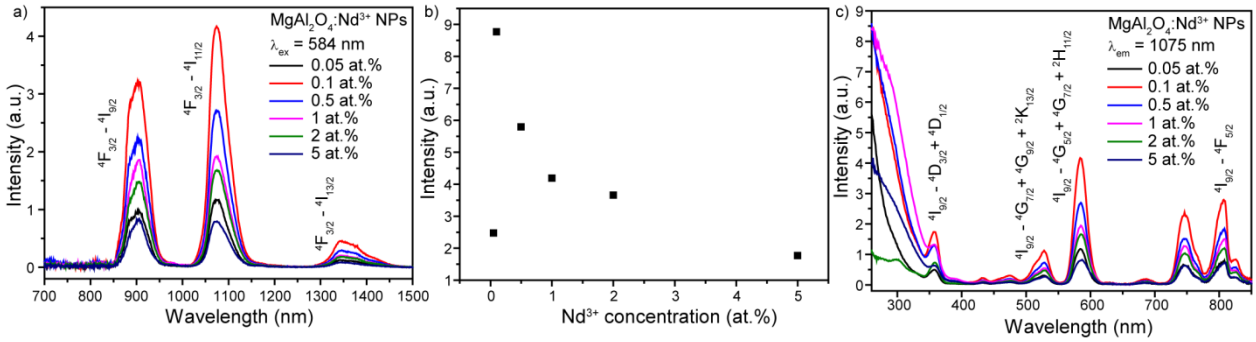

Fig. 3. a) Emission spectra of nanocrystalline $MgAl_2O_4:Nd^{3+}$ phosphors (λ_{ex} = 584 nm), b) concentration dependence of $^4F_{3/2}$ – $^4I_{11/2}$ transition intensity, c) excitation spectra of nanocrystalline $MgAl_2O_4:Nd^{3+}$ phosphors (λ_{em} = 1075 nm)

Fig. 4a shows luminescence decays of nanocrystalline $MgAl_2O_4:Nd^{3+}$ concentration series monitored at $^4F_{3/2}$ – $^4I_{11/2}$ transition upon 584 nm excitation. Noteworthy, that experimental data of samples doped with 0.05, 0.1 and 0.5 at.% were fitted by mono-exponential function, whereas higher doped samples required biexponential model to provide correct fitting. In the latter case the average lifetime was obtained according following formula [34]:

$$\tau_{av} = \frac{A_1\tau_1^2 + A_2\tau_2^2}{A_1\tau_1 + A_2\tau_2} \quad (1)$$

where A_1 and A_2 are pre-exponential factors; τ_1 and τ_2 are lifetimes. The change of fitting function can be explained using two hypotheses. The first hypothesis takes into account two non-equivalent sites for substitution in $MgAl_2O_4$ host. The dopant ions replace mainly Mg^{2+} sites in the crystal lattice due to the smaller differences between their ionic radii than in case of Al^{3+} ions, however, the Al^{3+} sites could also be replaced [10,23]. It can be assumed that Nd^{3+} ions situated at Mg^{2+} sites in the low-doped samples, while growth of doping concentration results in additional substitution of Al^{3+} sites, which leads to biexponential luminescence decay. The second hypothesis is focused on nanometer size of studied objects. Doping concentration increase leads to growth of Nd^{3+} doping ions located on the nanoparticles surface. It is well-know that decay rates of the lanthanide ions situated at the surface and in the volume of the nanoparticles demonstrate different decay rates [35,36]. The obtained Nd^{3+} lifetimes as a function of doping concentration are presented in Fig. 4b. One can see that the lifetime gradually declines from 181 μs to 88 μs along with increase of Nd^{3+} ions number.

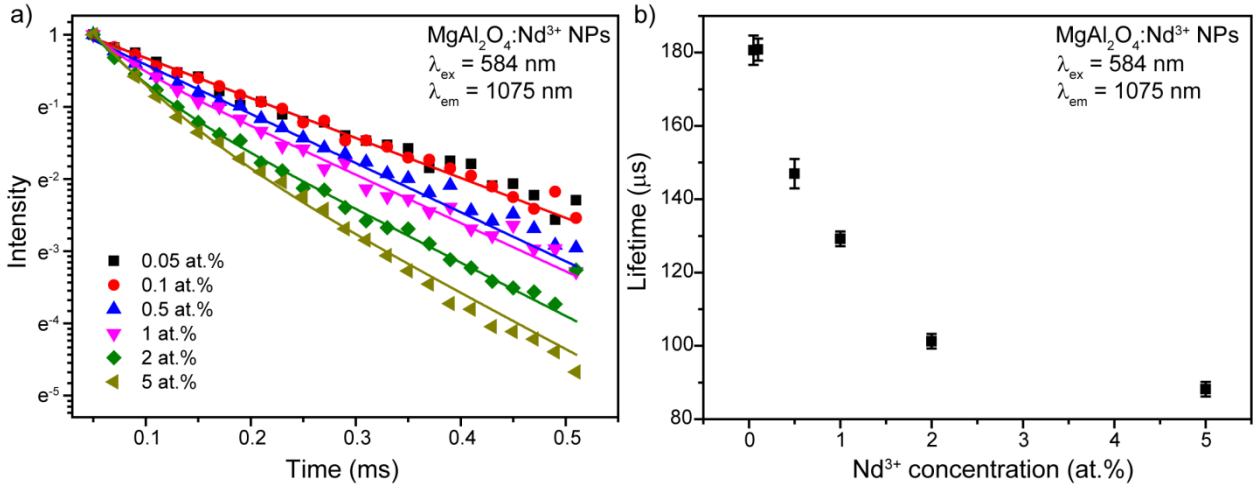

Fig. 4. a) Decay curves of $MgAl_2O_4:Nd^{3+}$ nanophosphors (λ_{ex}=584 nm; λ_{em}=1075 nm), (b) $^4F_{3/2}$ level lifetime of Nd^{3+} ions as a function of Nd^{3+} doping concentration

It was previously observed that concentration quenching starts from 0.1 at.% in spinel host [24]. As majority of Nd^{3+} ions locate at Mg^{2+} sites, the energy transfer mechanism can be defined by the critical energy transfer distance (R_c) according to Blasse et al. The critical energy transfer distance was calculated by the following equation [37]:

$$R_c \approx 2\left[\frac{3V}{4\pi x_c N}\right]^{1/3} \quad (2)$$

where x_c is the critical doping content (x_c = 0.001), N is the number of cation sites in the unit cell (N = 8 for $MgAl_2O_4$), and V is the volume of the unit cell ($V \approx 520$ Å^3). As calculated value of R_c (49.9 Å) is bigger than 5 Å, so exchange interaction cannot control energy transfer between Nd^{3+} ions in spinel host [38]. Therefore, it can be concluded that the concentration quenching is caused by the multipolar interaction mechanism [39,40]. Multipolar interaction includes dipole–dipole (d–d), dipole–quadrupole (d–q), and quadrupole–quadrupole (q–q) interaction. An interaction type can be determined using formula proposed by Van Uitert [41]. Further, Ozawa and Jaffe modified it as follows [42]:

$$\frac{I}{x} = k\left[1 + \beta(x)^{\theta/3}\right]^{-1} \quad (3)$$

where I is the integral intensity, x is the activator concentration, k and β are constant for the same excitation conditions for a given host crystal. According to the above equation θ = 3 for the energy transfer among the nearest neighbor ions, while θ = 6, 8 and 10 for d–d, d–q and q–q interactions, respectively [43,44].

The doping concentration effect on the emission intensity of $MgAl_2O_4:Nd^{3+}$ nanocrystalline phosphors was studied using the above theory. The multipolar character (θ) can be obtained by plotting log (I/x) vs log (x) as shown in Fig. 5. The slope θ/3 from approximation was determined to be -1.39, giving calculated value of θ is closer to 3. Therefore, we can conclude that concentration quenching in $MgAl_2O_4:Nd^{3+}$ samples occurred via energy transfer among the nearest neighbor ions.

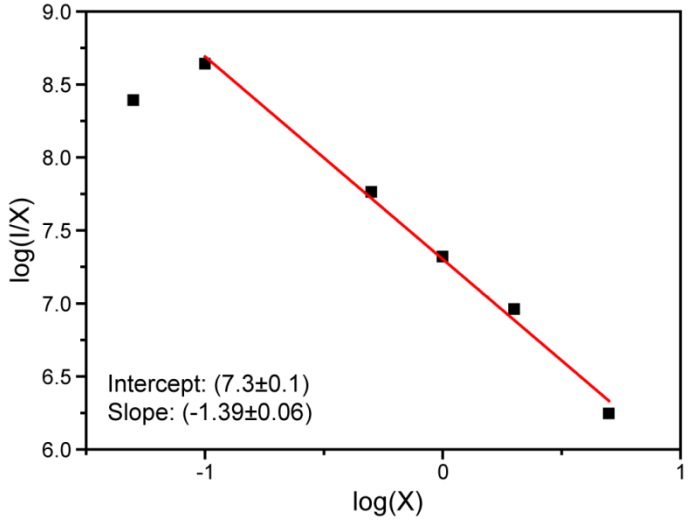

Fig. 5. Relation between log(I/x) and log (x) in $MgAl_2O_4:Nd^{3+}$ nanocrystalline phosphors. Line is a linear fit

4. Conclusions

To study the effect of neodymium concentration on the spectral characteristics of $MgAl_2O_4:Nd^{3+}$ powder, we synthesized a series of samples via modified Pechini method. The prepared samples were investigated using various experimental techniques. Based on the results of X-Ray diffraction, the spatial symmetry group of Fd-3m, the unit cell volume of (520±2) Å ^{3}, and the lattice parameter of 8.04 Å were determined for $MgAl_2O_4:Nd^{3+}$ 0.1 at.% nanophosphor. Scanning electron microscopy showed that $MgAl_2O_4:Nd^{3+}$ 0.1 at.% powder consists uniform spherical particles with the average size less than 100 nm. Energy-dispersive spectroscopy confirmed presence of O (51.68 %), Mg (16.23 %) and Al (32.08 %) in $MgAl_2O_4:Nd^{3+}$ 0.1 at.% sample. Photoluminescence characteristics of Nd^{3+}-doped $MgAl_2O_4$ concentration series was studied using steady-state and kinetics measurements. Emission spectra demonstrated three electronic transition $^4F_{3/2}$–$^4I_{9/2}$, $^4F_{3/2}$–$^4I_{11/2}$, $^4F_{3/2}$–$^4I_{13/2}$ situated in the near IR region. The most prominent emission line centered at 1075 nm is attributed to the transition $^4F_{3/2}$–$^4I_{11/2}$. Excitation spectra consisted of intense broad charge transfer band and series of intra-configurational f-f transitions. The optimal Nd^{3+} doping concentration was found to be 0.1 at.% in $MgAl_2O_4$ host. Growth of doping concentration led to monotonic $^4F_{3/2}$ lifetime decrease. Concentration quenching in $MgAl_2O_4:Nd^{3+}$ phosphors occurred via energy transfer among the nearest neighbor ions.

Acknowledgments

This research work was supported by the Academic Excellence Project 5-100 proposed by Peter the Great St. Petersburg Polytechnic University. Experimental measurements were performed in "Center for Optical and Laser materials research", "Research Centre for X-ray Diffraction Studies", and "Interdisciplinary Resource Center for Nanotechnology" (St. Petersburg State University).

References

[1] H. Gong, D. Tang, H. Huang, J. Ma, Agglomeration control of Nd: YAG nanoparticles via freeze drying for transparent Nd: YAG ceramics, J. Am. Ceram. Soc. 92 (2009) 812–817.
[2] B.R. Judd, Optical absorption intensities of rare-earth ions, Phys. Rev. 127 (1962) 750.
[3] D.A. Giljohann, D.S. Seferos, W.L. Daniel, M.D. Massich, P.C. Patel, C.A. Mirkin, Gold nanoparticles for biology and medicine, Angew. Chemie Int. Ed. 49 (2010) 3280–3294.
[4] O. V Salata, Applications of nanoparticles in biology and medicine, J. Nanobiotechnology. 2 (2004) 3.
[5] E.M.M. Ewais, A.A.M. El-Amir, D.H.A. Besisa, M. Esmat, B.E.H. El-Anadouli, Synthesis of nanocrystalline MgO/MgAl2O4 spinel powders from industrial wastes, J. Alloys Compd. 691 (2017) 822–833.
[6] C. Feldmann, T. Jüstel, C.R. Ronda, P.J. Schmidt, Inorganic Luminescent Materials: 100 Years of Research and Application, Adv. Funct. Mater. 13 (2003) 511–516. https://doi.org/10.1002/adfm.200301005.
[7] A. Steinegger, I. Klimant, S.M. Borisov, Purely organic dyes with thermally activated delayed fluorescence—a versatile class of indicators for optical temperature sensing, Adv. Opt. Mater. 5 (2017) 1700372.
[8] I. Omkaram, S. Buddhudu, Photoluminescence properties of MgAl2O4: Dy3+ powder phosphor, Opt. Mater. (Amst). 32 (2009) 8–11.
[9] Y. Zhang, Z. Guo, Z. Han, X. Xiao, Effect of rare earth oxides doping on MgAl2O4 spinel obtained by sintering of secondary aluminium dross, J. Alloys Compd. 735 (2018) 2597–2603.
[10] E.V. Golyeva, I.E. Kolesnikov, E. Lähderanta, A.V. Kurochkin, M.D. Mikhailov, Effect

of synthesis conditions on structural, morphological and luminescence properties of MgAl<inf>2</inf>O<inf>4</inf>:Eu^{3+}nanopowders, J. Lumin. 194 (2018). https://doi.org/10.1016/j.jlumin.2017.10.068.
[11] I.E. Kolesnikov, E.V. Golyeva, A.V. Kurochkin, M.D. Mikhailov, Structural and luminescence properties of MgAl2O4:Eu3+ nanopowders, J. Alloys Compd. 654 (2016) 32–38. https://doi.org/10.1016/j.jallcom.2015.09.122.
[12] E.M. Yoshimura, C.N. Santos, A. Ibanez, A.C. Hernandes, Thermoluminescent and optical absorption properties of neodymium doped yttrium aluminoborate and yttrium calcium borate glasses, Opt. Mater. (Amst). 31 (2009) 795–799.
[13] S. Geller, H.J. Williams, R.C. Sherwood, Magnetic and crystallographic study of neodymium-substituted yttrium and gadolinium iron garnets, Phys. Rev. 123 (1961) 1692.
[14] C. Zaldo, Lanthanide-based luminescent thermosensors: From bulk to nanoscale, in: Lanthanide-Based Multifunct. Mater., Elsevier, 2018: pp. 335–379.
[15] H.T. Amorim, M. V.D. Vermelho, A.S. Gouveia-Neto, F.C. Cassanjes, S.J.L. Ribeiro, Y. Messaddeq, Energy upconversion luminescence in neodymium-doped tellurite glass, J. Alloys Compd. 346 (2002) 282–284. https://doi.org/10.1016/S0925-8388(02)00513-3.
[16] E.M.M. Ewais, D.H.A. Besisa, A.A.M. El-Amir, S.M. El-Sheikh, D.E. Rayan, Optical properties of nanocrystalline magnesium aluminate spinel synthesized from industrial wastes, J. Alloys Compd. 649 (2015) 159–166.
[17] U. Önen, T. Boyraz, Microstructural characterization and thermal properties of aluminium titanate/spinel ceramic matrix composites, Acta Phys. Pol. A. 125 (2014) 488–490.
[18] M.Y. Nassar, I.S. Ahmed, I. Samir, A novel synthetic route for magnesium aluminate (MgAl2O4) nanoparticles using sol–gel auto combustion method and their photocatalytic properties, Spectrochim. Acta Part A Mol. Biomol. Spectrosc. 131 (2014) 329–334.
[19] J. Zhang, T. Lu, X. Chang, N. Wei, J. Qi, Unique mechanical properties of nanostructured transparent MgAl 2 O 4 ceramics, Nanoscale Res. Lett. 8 (2013) 261.
[20] M.E. Foley, R.W. Meulenberg, J.R. McBride, G.F. Strouse, Eu3+-doped ZnB2O4 (B= Al3+, Ga3+) nanospinels: an efficient red phosphor, Chem. Mater. 27 (2015) 8362–8374.
[21] D.A. Hardy, R.A. Tigaa, J.R. McBride, R.E. Ortega, G.F. Strouse, Structure–function correlation: Engineering high quantum yields in down-shifting nanophosphors, J. Am. Chem. Soc. 141 (2019) 20416–20423.
[22] I. V Beketov, A.I. Medvedev, O.M. Samatov, A. V Spirina, K.I. Shabanova, Synthesis and luminescent properties of MgAl2O4: Eu nanopowders, J. Alloys Compd. 586 (2014) S472–S475.
[23] R.J. Wiglusz, T. Grzyb, a. Lukowiak, P. Głuchowski, S. Lis, W. Strek, Comparative studies on structural and luminescent properties of Eu3+:MgAl2O4 and Eu3+/Na+:MgAl2O4 nanopowders and nanoceramics, Opt. Mater. (Amst). 35 (2012) 130–135. https://doi.org/10.1016/j.optmat.2012.07.017.
[24] P.J. Dereń, K. Maleszka-Bagińska, P. Głuchowski, M. a. Małecka, Spectroscopic properties of Nd3+ in MgAl2O4 spinel nanocrystals, J. Alloys Compd. 525 (2012) 39–43. https://doi.org/10.1016/j.jallcom.2012.02.065.
[25] R. Boulesteix, A. Maître, K. Lemański, P.J. Dereń, Structural and spectroscopic properties of MgAl2O4:Nd3+ transparent ceramics fabricated by using two-step Spark Plasma Sintering, J. Alloys Compd. 722 (2017) 358–364. https://doi.org/10.1016/j.jallcom.2017.06.101.
[26] I.E. Kolesnikov, E.V. Golyeva, E. Lähderanta, A.V. Kurochkin, M.D. Mikhailov, Ratiometric thermal sensing based on Eu^{3+}-doped YVO<inf>4</inf> nanoparticles, J. Nanoparticle Res. 18 (2016). https://doi.org/10.1007/s11051-016-3675-8.
[27] D. V Mamonova, I.E. Kolesnikov, A.A. Manshina, M.D. Mikhailov, V.M. Smirnov, Modified Pechini method for the synthesis of weakly-agglomerated nanocrystalline yttrium aluminum garnet (YAG) powders, Mater. Chem. Phys. 189 (2017) 245–251.
[28] I.E. Kolesnikov, M.A. Kurochkin, A.A. Kalinichev, D.V. Mamonova, E.Y. Kolesnikov,

A.V. Kurochkin, E. Lähderanta, M.D. Mikhailov, Effect of silica coating on luminescence and temperature sensing properties of Nd3+doped nanoparticles, J. Alloys Compd. 734 (2018) 136–143. https://doi.org/10.1016/j.jallcom.2017.11.048.
[29] I.E. Kolesnikov, A.A. Kalinichev, M.A. Kurochkin, D. V. Mamonova, E.Y. Kolesnikov, E. Lähderanta, M.D. Mikhailov, Bifunctional heater-thermometer Nd 3+ -doped nanoparticles with multiple temperature sensing parameters, Nanotechnology. 30 (2019) 145501. https://doi.org/10.1088/1361-6528/aafcb8.
[30] W. Strek, P. Dereń, A. Bednarkiewicz, M. Zawadzki, J. Wrzyszcz, Emission properties of nanostructured Eu 3+ doped zinc aluminate spinels, J. Alloys Compd. 300 (2000) 456–458.
[31] I.E. Kolesnikov, E. V. Golyeva, E. V. Borisov, E.Y. Kolesnikov, E. Lähderanta, A. V. Kurochkin, M.D. Mikhailov, Photoluminescence properties of Eu3+-doped MgAl2O4 nanoparticles in various surrounding media, J. Rare Earths. 37 (2019) 806–811. https://doi.org/10.1016/j.jre.2018.10.019.
[32] C. Hang, Z. Pei-Fen, Z. Hong-Yang, L. Hong-Dong, C. Qi-Liang, Photoluminescence properties and energy transfer in Y2O3: Eu3+ nanophosphors, Chinese Phys. B. 23 (2014) 57801.
[33] J.B. Gruber, D.K. Sardar, K.L. Nash, R.M. Yow, Comparative study of the crystal-field splitting of trivalent neodymium energy levels in polycrystalline ceramic and nanocrystalline yttrium oxide, J. Appl. Phys. 102 (2007) 23103.
[34] T. Fujii, K. Kodaira, O. Kawauchi, N. Tanaka, H. Yamashita, M. Anpo, Photochromic behavior in the fluorescence spectra of 9-anthrol encapsulated in Si-Al glasses prepared by the sol-gel method, J. Phys. Chem. B. 101 (1997) 10631–10637.
[35] N.S. Singh, R.S. Ningthoujam, M.N. Luwang, S.D. Singh, R.K. Vatsa, Luminescence, lifetime and quantum yield studies of YVO4: Ln3+ (Ln3+= Dy3+, Eu3+) nanoparticles: Concentration and annealing effects, Chem. Phys. Lett. 480 (2009) 237–242.
[36] I.E. Kolesnikov, D.V. Mamonova, E. Lähderanta, A.V. Kurochkin, M.D. Mikhailov, The impact of doping concentration on structure and photoluminescence of Lu2O3:Eu3+ nanocrystals, J. Lumin. 187 (2017) 26–32. https://doi.org/10.1016/j.jlumin.2017.03.006.
[37] G. Blasse, A. Bril, A NEW PHOSPHOR FOR FLYING-SPOT CATHODE-RAY TUBES FOR COLOR TELEVISION: YELLOW-EMITTING Y3Al5O12–Ce3+, Appl. Phys. Lett. 11 (1967) 53–55.
[38] R. Naik, S.C. Prashantha, H. Nagabhushana, S.C. Sharma, B.M. Nagabhushana, H.P. Nagaswarupa, H.B. Premkumar, Low temperature synthesis and photoluminescence properties of red emitting Mg2SiO4:Eu3+ nanophosphor for near UV light emitting diodes, Sensors Actuators B Chem. 195 (2014) 140–149. https://doi.org/10.1016/j.snb.2014.01.018.
[39] G. Blasse, Energy transfer in oxidic phosphors, Phys. Lett. A. 28 (1968) 444–445. https://doi.org/10.1016/0375-9601(68)90486-6.
[40] D. Chikte, S.K. Omanwar, S. V Moharil, Luminescence properties of red emitting phosphor NaSrBO3: Eu3+ prepared with novel combustion synthesis method, J. Lumin. 142 (2013) 180–183.
[41] L.G. Van Uitert, Characterization of Energy Transfer Interactions between Rare Earth Ions, J. Electrochem. Soc. 114 (1967) 1048. https://doi.org/10.1149/1.2424184.
[42] L. Ozawa, P.M. Jaffe, Mechanism of Emission Color Shift with Activator Concentration in Eu+3 Activated Phosphors, J. Electrochem. Soc. 118 (1971) 1678–1979.
[43] L. Ozawa, Determination of Self-Concentration Quenching Mechanisms of Rare Earth Luminescence from Intensity Measurements on Powdered Phosphor Screens, J. Electrochem. Soc. 126 (1979) 106–109.
[44] F. Yang, Z. Yang, Q. Yu, Y. Liu, X. Li, F. Lu, Sm 3+-doped Ba 3 Bi (PO 4) 3 orange reddish emitting phosphor, Spectrochim. Acta Part A Mol. Biomol. Spectrosc. 105 (2013) 626–631.